

Anti-Critical Quantum Metrology

George Mihailescu  ^{1,2} and Karol Gietka  ^{3,*}

¹*School of Physics, University College Dublin, Belfield, Dublin 4, Ireland*

²*Centre for Quantum Engineering, Science, and Technology, University College Dublin, Dublin 4, Ireland*

³*Institut für Theoretische Physik, Universität Innsbruck, Technikerstraße 21a, A-6020 Innsbruck, Austria*

(Dated: February 4, 2026)

Critical quantum metrology exploits the dramatic growth of the quantum Fisher information near quantum phase transitions to enhance the precision of parameter estimation. Traditionally, this enhancement is associated with a closing energy gap, which causes the characteristic timescales for adiabatic preparation or relaxation to diverge with increasing system size. Consequently, the apparent growth of the quantum Fisher information largely reflects the increasing evolution time induced by critical slowing down, rather than a genuine gain in metrological performance, thereby severely limiting the practical usefulness of such protocols. Here we show that the relationship between energy-gap variations, quantum Fisher information, and achievable precision is far more subtle in interacting quantum systems: enhanced sensitivity does not require a vanishing gap, and, perhaps more surprisingly, a decreasing quantum Fisher information does not necessarily imply reduced precision once the time is properly taken into account. Building on this insight, we introduce an anti-critical metrology scheme that achieves enhanced precision while the energy gap increases. We illustrate this mechanism using the quantum Rabi model, thereby identifying a route to metrological advantage that avoids the critical slowing down associated with conventional criticality.

I. INTRODUCTION

Quantum metrology seeks to exploit the laws of quantum mechanics to estimate physical parameters with the highest possible precision [1, 2]. Quantum correlations can be used to surpass the standard quantum limit of precision achievable with separable states, reaching in principle the Heisenberg limit [3–5]. Despite tremendous experimental and theoretical progress, overcoming the standard quantum limit in macroscopic quantum systems remains largely elusive [6–11]. The reason is that strongly correlated many-body quantum states are difficult to prepare and are extremely fragile to noise and decoherence [12, 13]. This has motivated the search for new approaches, and over the past decade critical quantum metrology has emerged as a particularly promising direction [14–17]. By tuning a system close to a quantum phase transition, the closing of the many-body energy gap and the associated build-up of quantum correlations lead to extreme sensitivity, as witnessed by the quantum Fisher information. In some situations, this sensitivity can be more robust than in conventional approaches to quantum metrology [18–21]. However, the same gap closing that enhances the quantum Fisher information also induces critical slowing down: the timescales required to prepare, transform, probe, or read out the system diverge, severely limiting practical applications. As a result, the apparent advantage of a large quantum Fisher information is often offset by prohibitively long evolution and preparation times [22]. This issue is particularly acute in the frequentist paradigm, where a large number of independent repetitions are required to approach the Cramér–Rao bound, effectively amplifying the time cost associated with each trial.

In this work, we challenge the prevailing intuition that closing energy gaps are required for quantum-enhanced metrology

in interacting quantum systems [23]. We carefully distinguish between the quantum Fisher information, which quantifies the sensitivity of a quantum state to variations of the estimated parameter, and the operationally relevant estimation precision, which must additionally account for the total time required to prepare and interrogate the probe state [24]. While a vanishing gap indeed guarantees a large quantum Fisher information, high estimation precision can also be achieved when the gap remains finite or even increases. In certain interacting systems, it can even be advantageous to deliberately seek a constant, rather than diverging, quantum Fisher information. This counterintuitive regime arises when the opening of the energy gap—largely overlooked in previous studies—plays the central role. Unlike in critical metrology, where enhanced sensitivity emerges at the cost of critical slowing down, here the system develops strong quantum correlations while remaining fast enough to equilibrate and enable measurements on short timescales. This leads to a form of anti-critical metrology that circumvents critical slowing down without sacrificing metrological performance. In other words, the anti-critical metrology relies on building the correlations and simultaneously opening the energy gap. We illustrate this concept using the finite-component phase transition in the quantum Rabi model [25], which can be mapped onto a pedagogical harmonic oscillator and has been extensively studied in the context of critical quantum metrology [26–30]. While we focus on the quantum Rabi model for concreteness, the mechanism underlying anti-critical metrology relies only on the interplay between interaction-induced squeezing and gap engineering and is therefore not restricted to integrable or few-mode systems. Nevertheless, its applicability is constrained by the fact that not all interacting systems admit controllable gap opening.

* karol.gietka@uibk.ac.at

II. QUANTUM RABI MODEL

To illustrate the idea of anti-critical metrology, we consider the quantum Rabi model [31], which is one of the simplest models exhibiting a finite-component quantum phase transition [25, 32]. Originally introduced to describe light–matter interactions in cavity quantum electrodynamics, the quantum Rabi model focuses on a single mode of the electromagnetic field interacting with a two-level system. However, it is a universal model for a harmonic oscillator coupled to a two-level system and can be realized in a wide variety of physical platforms, including trapped ions [33, 34], circuit quantum electrodynamics [35], and ultracold atoms [36]. The Hamiltonian of the quantum Rabi model reads ($\hbar \equiv 1$)

$$\hat{H} = \omega \hat{a}^\dagger \hat{a} + \frac{\Omega}{2} \hat{\sigma}_z + \frac{g}{2} (\hat{a} + \hat{a}^\dagger) \hat{\sigma}_x, \quad (1)$$

where ω is the frequency of the harmonic oscillator, Ω is the energy splitting of the two-level system, g is the light–matter coupling strength, \hat{a} and \hat{a}^\dagger are the bosonic annihilation and creation operators, and $\hat{\sigma}_x$ and $\hat{\sigma}_z$ are Pauli matrices acting on the two-level system.

In this work, we focus on the finite-component phase transition that emerges in the regime where the two-level splitting is much larger than the oscillator frequency, $\Omega \gg \omega$ [25]. In this limit, the hierarchy of energy scales effectively suppresses spin flips and renders the spin degree of freedom increasingly rigid. As a result, the ratio Ω/ω plays a role analogous to a thermodynamic limit. When $\Omega/\omega \rightarrow \infty$, the nonanalytic behavior can develop even though the system contains only a single two-level component and an oscillator. In this regime, the dynamics are accurately captured by an effective Hamiltonian obtained through a perturbative expansion in ω/Ω . To leading order, one finds

$$\hat{H}_{\text{eff}} = \omega \hat{a}^\dagger \hat{a} + \frac{\Omega}{2} \hat{\sigma}_z + \frac{g^2}{4\Omega} (\hat{a} + \hat{a}^\dagger)^2 \hat{\sigma}_z + \mathcal{O}\left(\frac{\omega}{\Omega}\right), \quad (2)$$

which already captures the essential features of a quantum phase transition like closing energy gap and the built-up of correlations.

For the low energy spin down sector (effectively replacing $\hat{\sigma}_z$ with -1) we obtain up to constant terms

$$\hat{H} \approx \omega \hat{a}^\dagger \hat{a} - \frac{g^2}{4\Omega} (\hat{a} + \hat{a}^\dagger)^2, \quad (3)$$

which corresponds to a single-mode squeezing Hamiltonian or equivalently an opening harmonic oscillator when expressed in the diagonal form

$$\hat{H} \approx \omega \sqrt{1 - \frac{g^2}{\omega \Omega}} \hat{c}^\dagger \hat{c}, \quad (4)$$

where $\hat{c} = \hat{a} \cosh \xi_- - \hat{a}^\dagger \sinh \xi_-$ with $\xi_- \equiv -\frac{1}{4} \log(1 - g^2/g_c^2)$.

The finite-component quantum phase transition occurs when the coefficient in front of $(\hat{a} + \hat{a}^\dagger)^2$ reaches the critical value at $g = g_c \equiv \sqrt{\omega \Omega}$ at which the effective oscillator frequency $\omega \sqrt{1 - g^2/g_c^2}$ vanishes, leading to a closing of the

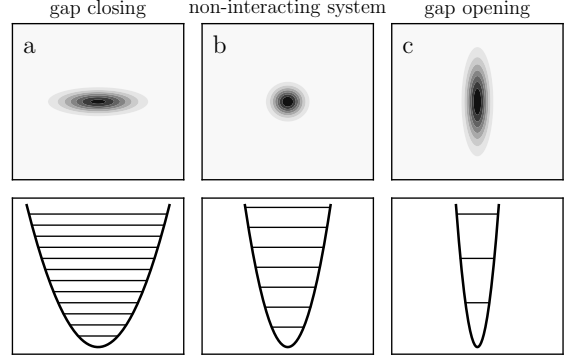


FIG. 1. Schematic illustrating the concepts of critical and anti-critical metrology. Top panels represent the phase space ground state of the associated potentials depicted in the bottom panel. Starting from the non-interacting spectrum and a corresponding vacuum state (b), interactions can close the energy gap—realizing critical metrology (a)—or open it—realizing anti-critical metrology (c). In both cases the final state is squeezed, but the relevant timescales differ dramatically. In critical metrology, a vanishing gap lengthens the timescales, artificially enhancing the quantum Fisher information, whereas in anti-critical metrology, a growing gap shortens them, artificially suppressing the quantum Fisher information. This behavior reflects the fact that, in many interacting quantum systems, the energy gap—and thus the characteristic timescales—scale with the system size.

energy gap. While conventional critical metrology would operate in the vicinity of this critical point [29, 36, 37], where the quantum Fisher information diverges, the anti-critical approach deliberately avoids the critical point and the associated critical slowing down. Instead, we engineer parameter regimes in which the correlations as well as the estimation precision increase while the effective energy gap becomes larger. This allows us to retain the metrological enhancement of correlated states without the detrimental scaling of timescales (see Fig. 1 for a schematic illustration). In the following, we revise the critical metrology approach and then introduce the anti-critical metrology protocol.

III. CRITICAL METROLOGY

The central figure of merit in quantum metrology—and naturally in critical metrology—is the aforementioned quantum Fisher information, which determines the ultimate precision of parameter estimation via the Cramér–Rao bound [8, 38, 39]. For pure states the quantum Fisher information admits a simple form

$$\mathcal{I}_\omega = 4 \left(\langle \partial_\omega \psi | \partial_\omega \psi \rangle - |\langle \partial_\omega \psi | \psi \rangle|^2 \right), \quad (5)$$

where the derivative is taken with respect to the parameter of interest, here the frequency ω . Critical metrology typically exploits the sensitivity of the ground state near a quantum phase transition. In the quantum Rabi model, deep in the $\Omega \gg \omega$

limit, the ground state reduces to a squeezed vacuum

$$|\psi\rangle = \exp\left[\frac{\xi_-}{2}(\hat{a}^2 + \hat{a}^{\dagger 2})\right]|0\rangle, \quad (6)$$

with squeezing parameter $\xi_- \equiv -\frac{1}{4}\log(1 - g^2/g_c^2)$. This parameter is directly linked to the frequency of the effective harmonic oscillator [40], $\omega\sqrt{1 - g^2/g_c^2} = \omega e^{-2\xi_-}$, so approaching the critical point both enhances squeezing—well known to boost precision—and simultaneously closes the spectral gap, thereby inducing long timescales [41–44] (See Fig. 1a).

Evaluating the quantum Fisher information for this squeezed ground state yields

$$\mathcal{I}_\omega = 2(\partial_\omega \xi_-)^2 = \frac{g^4/g_c^4}{8\omega^2(1 - g^2/g_c^2)^2}. \quad (7)$$

Although the quantum Fisher information explodes at $g = g_c$, the expression obtained above is written solely in terms of Hamiltonian parameters. In this form it does not yet quantify the physical resources involved such as the number of excitations or the time required to prepare the state. In particular, the bare formula seems to suggest that the quantum Fisher information could be increased or decreased at will simply by tuning ω , without modifying the excitation content of the state or introducing additional correlations. The resolution lies in the fact that the quantum Fisher information implicitly depends on the time required either to adiabatically transform the ground state into one corresponding to a slightly different parameter value [22] or to relax from an excited state—timescales that are ultimately set by the energy gap.

To make this explicit, consider first the mean excitation number in the squeezed vacuum,

$$\langle \hat{a}^\dagger \hat{a} \rangle = \sinh^2 \xi_- \approx \frac{1}{4\sqrt{1 - g^2/g_c^2}}, \quad (8)$$

where the approximation holds near the critical point $g \approx g_c$ and depends on the ratio g/g_c . Next, the transformation time is constrained by the closing of the energy gap [22, 41–43, 45]. For an adiabatic sweep from $g/g_c \approx 1 - \delta$ (with $\delta \ll 1$) toward the critical point $g/g_c \approx 1$, the minimal evolution time scales as

$$T \sim \frac{1}{\omega\sqrt{1 - g^2/g_c^2}}. \quad (9)$$

Thus, both the excitation number and the evolution time inherit the same critical dependence on the parameters of the system. Substituting these relations into the quantum Fisher information gives [29]

$$\mathcal{I}_\omega \sim \langle \hat{a}^\dagger \hat{a} \rangle^2 T^2, \quad (10)$$

showing that the apparent divergence of the quantum Fisher information is entirely accounted for by Heisenberg scaling with respect to the excitation number (as is characteristic for squeezed states) and with respect to the transformation time. An alternative derivation is provided in Appendix A.

An equivalent viewpoint is provided by the effective harmonic oscillator picture [Eq. (4)] relevant for the ultra-strong

coupling regime [21, 46, 47] where the environment is coupled to the system through its eigenstates related to \hat{c} instead of eigenstates of the non-interacting oscillator represented by \hat{a} [48–50]. Here, one estimates ω from the response of an oscillator with re-normalized frequency $\omega\sqrt{1 - g^2/g_c^2}$ described by the associated operators \hat{c} and \hat{c}^\dagger . In this setting a quantum state $|\psi\rangle$ evolves according to

$$|\psi(t)\rangle = \exp\left[-it\hat{c}^\dagger \hat{c} \omega\sqrt{1 - g^2/g_c^2}\right]|\psi\rangle \quad (11)$$

and the quantum Fisher information takes the form

$$\mathcal{I}_\omega = 4t^2 \Delta^2 \hat{c}^\dagger \hat{c} \left(\partial_\omega \omega\sqrt{1 - g^2/g_c^2}\right)^2, \quad (12)$$

where t is the free evolution time (not related to T or the energy gap) of the effective oscillator and $\Delta^2 \hat{c}^\dagger \hat{c}$ characterizes the initial state: for instance, for a coherent state, one obtains $\Delta^2 \hat{c}^\dagger \hat{c} = |\alpha|^2$. Near criticality, the derivative of the effective frequency becomes

$$\left(\partial_\omega \omega\sqrt{1 - g^2/g_c^2}\right)^2 = \frac{(2 - g^2/g_c^2)^2}{4(1 - g^2/g_c^2)} \approx 4\langle \hat{a}^\dagger \hat{a} \rangle^2, \quad (13)$$

so the scaling is again governed by the critical dependence on the parameters or the excitation number of the original mode \hat{a} . In practice, however, the vanishing gap implies arbitrarily long transformation or relaxation times. For instance, in driven-dissipative setups the steady-state relaxation time grows with the oscillator quality factor and inverse frequency [51].

To summarize, while the quantum Fisher information near criticality can be extremely large, it is inevitably constrained by critical slowing down. Indeed, the excitation number in the quantum Rabi model is proportional to the energy gap and therefore to the characteristic time required to transform the ground state or to equilibrate:

$$\langle \hat{a}^\dagger \hat{a} \rangle \sim \omega T. \quad (14)$$

In the next section, we turn to an alternative approach where this trade-off takes on a different and more favorable form.

IV. ANTI-CRITICAL METROLOGY

The central idea of anti-critical metrology is to deliberately open, or more generally engineer, the energy gap in order to obtain favorable scaling of estimation precision. In the context of the quantum Rabi model (see Appendix D and F for alternative models), one can achieve such an opening by considering the high-energy sector and replacing $\hat{\sigma}_z \rightarrow +1$. The resulting effective Hamiltonian reads

$$\hat{H} \approx \omega \hat{a}^\dagger \hat{a} + \frac{g^2}{4\Omega}(\hat{a} + \hat{a}^\dagger)^2, \quad (15)$$

which is again a squeezing Hamiltonian. Its ground state is a squeezed vacuum,

$$|\psi\rangle = \exp\left[\frac{\xi_+}{2}(\hat{a}^2 + \hat{a}^{\dagger 2})\right]|0\rangle, \quad (16)$$

but with a different squeezing parameter $\xi_+ \equiv -\frac{1}{4} \log(1 + g^2/g_c^2)$. This corresponds to an effective harmonic oscillator

$$\hat{H} = \omega \sqrt{1 + g^2/g_c^2} \hat{c}^\dagger \hat{c} = \omega e^{-2\xi_+} \hat{c}^\dagger \hat{c}, \quad (17)$$

with a frequency that opens as the coupling strength g is increased. Thus squeezing is generated, but now at the cost—or rather at the benefit—of a growing energy gap (see Fig. 1c).

The quantum Fisher information associated with this ground state is

$$\mathcal{I}_\omega = 2(\partial_\omega \xi_+)^2 = \frac{g^4/g_c^4}{8\omega^2(1 + g^2/g_c^2)^2} \approx \frac{1}{8\omega^2}, \quad (18)$$

where the approximation holds for $g/g_c \gg 1$. From the perspective of achieving large quantum Fisher information, this result may appear disappointing. Despite creating strong squeezing, the quantum Fisher information does not increase with g but remains constant. Why is this the case? The essential point is that in anti-critical metrology the opening of the gap shortens all relevant timescales and eliminates thus the critical-slowness. To see why the quantum Fisher information remains constant, recall that for a squeezed vacuum it takes the form (see Appendix B)

$$\mathcal{I}_\omega \sim \langle \hat{a}^\dagger \hat{a} \rangle^2 T^2, \quad (19)$$

where T is the characteristic timescale related to the energy gap, as also evidenced in Eq. (10) (see also Appendix A, and C). Away from the critical point both the energy gap and the number of excitations grow with increasing g , implying that the timescale must decrease as $T \sim 1/\langle \hat{a}^\dagger \hat{a} \rangle$. As a result,

$$\mathcal{I}_\omega \sim \text{const.}, \quad (20)$$

so the quantum Fisher information does not increase with the number of excitations. The key insight is that, unlike in standard Ramsey interferometry, the time T is not a freely tunable resource, but is fixed by the underlying energy scales as well as the number of excitations.

This trade-off becomes explicit in the excitation number and timescale for the quantum Rabi model. The mean excitation number grows with coupling as

$$\langle \hat{a}^\dagger \hat{a} \rangle = \sinh^2 \xi_+ \approx \frac{1}{4} g/g_c, \quad (21)$$

valid for $g \gg g_c$, while the characteristic time decreases as

$$T \sim \frac{1}{\omega g/g_c} \sim \frac{1}{\omega \langle \hat{a}^\dagger \hat{a} \rangle}. \quad (22)$$

As a consequence, the quantum Fisher information becomes constant. See Fig. 2 for the comparison between critical and anti-critical approach without and with taking into account the adiabatic time related to transform a ground state into a neighboring ground state.

Although this compensation is not evident in Eq. (18), it is revealed clearly in the effective oscillator picture. There,

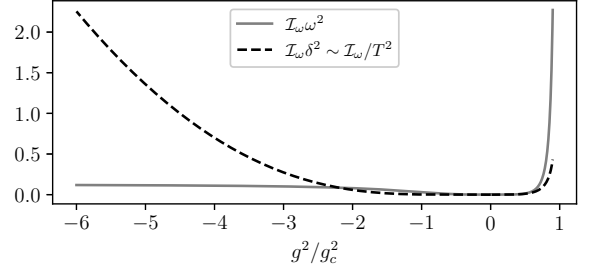


FIG. 2. Comparison between the quantum Fisher information (solid gray line) and the quantum Fisher information multiplied by the energy gap—equivalently, divided by the adiabatic time required to transform neighboring ground states (dashed black line). While the quantum Fisher information diverges near the critical point ($g^2/g_c^2 \approx 1$), accounting for the transformation time reveals that the sensitivity per unit time can be equally large away from criticality, where the required evolution time is much shorter due to the absence of critical slowing down. Exploiting the opening of the energy gap, and thus enabling an anti-critical metrology approach, may however require significantly stronger interactions. Simulations are performed using the effective description of the quantum Rabi model from Eq. (4) for $g^2/g_c^2 > 0$, and from Eq. (15) for $g^2/g_c^2 < 0$.

the derivative of the effective frequency with respect to the original frequency of interest scales as

$$\left(\partial_\omega \omega \sqrt{1 + g^2/g_c^2} \right)^2 \approx 4 \langle \hat{a}^\dagger \hat{a} \rangle^2, \quad (23)$$

which enhances the quantum Fisher information by a factor proportional to the excitation number [compare with Eq. (13)], while simultaneously reducing the relevant relaxation times as the energy gap increases. This mechanism realizes the protocol of anti-critical metrology, where squeezing is accompanied not by critical slowing down but by accelerated dynamics. Comparing the characteristic timescales (or, equivalently, energy scales), critical [Eq. (14)] and anti-critical [Eq. (22)], reveals that, for the quantum Rabi model, the anti-critical protocol attains the same scaling with the excitation number while being at least $\propto \langle \hat{a}^\dagger \hat{a} \rangle^2$ faster than the critical one.

V. CONCLUSIONS

In this work we have shown that in interacting quantum systems the quantum Fisher information does not necessarily need to diverge in order to achieve quantum-enhanced precision. This counter-intuitive result follows from the fact that in critical metrology the relevant timescales grow with approaching the critical point, while in anti-critical metrology they decrease by going away from the critical point. As a consequence, criticality leads to a naive enhancement of the sensitivity, whereas anti-criticality leads to a naive suppression. A careful accounting of resources—especially the time related to the energy gap—suggests that, for a given number of excitations, the anti-critical protocol might be advantageous, as it reaches the same sensitivity (per unit of time)

on significantly shorter characteristic timescales. To illustrate these principles we have considered the quantum Rabi model, a paradigmatic example of a finite-component quantum phase transition that has been extensively studied in the context of critical metrology. The same reasoning can be expected to carry over to a broad class of interacting systems, in particular to all-to-all-connected models [52] such as the Lipkin–Meshkov–Glick and Dicke models. One should keep in mind, however, that realizing the anti-critical protocol may require access to very strong interactions—potentially even stronger than those needed for critical metrology—but it offers the important conceptual insight that faster dynamics, rather than closing energy gap, can be the true resource for quantum-enhanced metrology. Nevertheless, not every interacting system would be suitable for anti-critical metrology as it relies on the gap opening (see Appendix E).

More broadly, our results suggest a new route for quantum metrology in interacting quantum systems that exploits gap opening and engineered spectra to simultaneously generate useful quantum correlations. This perspective seems to indicate that non-linear interactions, long-range couplings, or driven–dissipative mechanisms could be harnessed to design protocols in which enhanced precision arises not from critical slowing down, but from accelerated dynamics. In this context, finite-size systems appear particularly promising, as the amount of exploitable quantum correlations in an anti-critical metrology approach may be limited not by the energy gap, but rather by the finite dimensionality of the accessible Hilbert space [53]. At the same time, it is important to note that in certain situations critical metrology might still provide a better strategy. Nonetheless, the anti-critical approach opens a largely unexplored landscape of possibilities. Exploring such strategies—together with their practical challenges—may significantly expand the toolbox for implementing quantum-enhanced metrology in realistic interacting many-body platforms, while also deepening our understanding of the connection between quantum correlations and the energy gap in many-body quantum systems.

Appendix A: Quantum Fisher information for a harmonic oscillator ground state

Here we present an alternative calculation of the quantum Fisher information for the ground state of the quantum Rabi model (mapped to a harmonic oscillator). To this end, we use the following formula

$$\mathcal{I}_\omega = 4 \sum_{n \neq 0} \frac{|\langle \psi_n(\omega) | \partial_\omega \hat{H}(\omega) | \psi_0(\omega) \rangle|^2}{[E_n(\omega) - E_0(\omega)]^2}, \quad (\text{A1})$$

expressed through ω -dependent eigenstates $|\psi_n(\omega)\rangle$ and eigenvalues $E_n(\omega)$ of the Hamiltonian $\hat{H}(\omega)$. For the squeezed harmonic oscillator Hamiltonian

$$\hat{H} \approx \omega \hat{a}^\dagger \hat{a} \pm \frac{g^2}{4\Omega} (\hat{a} + \hat{a}^\dagger)^2, \quad (\text{A2})$$

where \pm indicates closing or opening the energy gap, it is straightforward to show that only one term from the sum over

n survives, leading to

$$\begin{aligned} \mathcal{I}_\omega &= \frac{|\langle \psi_2(\omega) | \hat{a}^\dagger \hat{a} | \psi_0(\omega) \rangle|^2}{\omega^2 (1 \pm g^2/g_c^2)} = \frac{2 \langle \hat{a}^\dagger \hat{a} \rangle (\langle \hat{a}^\dagger \hat{a} \rangle + 1)}{\omega^2 (1 \pm g^2/g_c^2)} \\ &= \frac{\Delta^2 \hat{a}^\dagger \hat{a}}{\omega^2 (1 \pm g^2/g_c^2)} \sim \langle \hat{a}^\dagger \hat{a} \rangle^2 T^2, \end{aligned} \quad (\text{A3})$$

where we have used the fact that $|\psi_n(\omega)\rangle = \exp\left[\frac{\xi_\omega}{2}(\hat{a}^\dagger)^2 - \hat{a}^2\right] |n\rangle$ and $T^{-2} \sim \omega^2 (1 \pm g^2/g_c^2)$ is related to the energy gap inverse squared. In both cases the quantum Fisher information exhibits quadratic (Heisenberg) scaling with the number of excitations $\langle \hat{a}^\dagger \hat{a} \rangle$ and time T which is related to the energy gap.

Since there is a mapping from the Lipkin–Meshkov–Glick model to a harmonic oscillator related to the Holstein–Primakoff transformation, the quantum Fisher information for the former can be expressed as

$$\mathcal{I}_\omega \approx \Delta^2 \hat{S}_z \delta^{-2}, \quad (\text{A4})$$

where $\delta = \omega \sqrt{1 - g/\omega}$, which can be seen in Fig. 3c.

Appendix B: Quantum Fisher information for a squeezed vacuum

For the sake of completeness, we show the quantum Fisher information for a squeezed vacuum $|\psi_0\rangle$ where the information about the unknown parameter ω is being imprinted through $\hat{H} = \omega \hat{a}^\dagger \hat{a}$ for time t . As a consequence the quantum Fisher information becomes

$$\mathcal{I}_\omega = 4t^2 \Delta^2 \hat{a}^\dagger \hat{a} = 4t^2 \times 2 \langle \hat{a}^\dagger \hat{a} \rangle (\langle \hat{a}^\dagger \hat{a} \rangle + 1), \quad (\text{B1})$$

where t is the free evolution time and is not related to the energy gap. This expression highlights two key points. First, the quantum Fisher information is directly enhanced by the number fluctuations of the squeezed state, its orientation does not matter. Second, it grows quadratically with the evolution time for a coherent process.

Appendix C: Quantum Fisher information for an adiabatic time evolution

We consider a family of Hamiltonians

$$\hat{H}(\omega, t) |\psi_n(t)\rangle = E_n(\omega, t) |\psi_n(t)\rangle, \quad (\text{C1})$$

depending smoothly on the parameter ω . The time evolution is governed by the time-ordered unitary

$$\hat{U}(\omega, T) = \mathcal{T} \exp\left[-i \int_0^T \hat{H}(\omega, t) dt\right]. \quad (\text{C2})$$

The generator of infinitesimal translations in ω is defined as

$$\hat{G}(\omega, T) = i \hat{U}^\dagger(\omega, T) \partial_\omega \hat{U}(\omega, T). \quad (\text{C3})$$

Exact integral representation of the generator

Differentiating the time-ordered exponential and using $\hat{U}(t, 0) = \mathcal{T}e^{-i\int_0^t \hat{H}(\omega, \tau) d\tau}$, one obtains the exact identity

$$\hat{G}(\omega, T) = \int_0^T \hat{U}^\dagger(t, 0) \partial_\omega \hat{H}(\omega, t) \hat{U}(t, 0) dt. \quad (\text{C4})$$

Introducing the Heisenberg-picture operator

$$\hat{A}_H(t) \equiv \hat{U}^\dagger(t, 0) \partial_\omega \hat{H}(\omega, t) \hat{U}(t, 0), \quad (\text{C5})$$

the generator can be written compactly as

$$\hat{G} = \int_0^T \hat{A}_H(t) dt. \quad (\text{C6})$$

Expectation value of the generator

We assume that the system is initially prepared in the instantaneous ground state $|\psi_0(0)\rangle$. The expectation value of the generator is then

$$\langle \hat{G} \rangle = \int_0^T \langle \psi_0(0) | \hat{A}_H(t) | \psi_0(0) \rangle dt. \quad (\text{C7})$$

Within the adiabatic approximation,

$$\hat{U}(t, 0) |\psi_n(0)\rangle \approx e^{-i\theta_n(t)} |\psi_n(t)\rangle, \quad (\text{C8})$$

where

$$\theta_n(t) = \int_0^t E_n(\tau) d\tau - i \int_0^t \langle \psi_n(\tau) | \partial_\tau \psi_n(\tau) \rangle d\tau \quad (\text{C9})$$

is the sum of the dynamical and Berry phases. This yields

$$\langle \hat{G} \rangle \approx \int_0^T \langle \psi_0(t) | \partial_\omega \hat{H}(\omega, t) | \psi_0(t) \rangle dt, \quad (\text{C10})$$

which coincides with the Feynman–Hellmann expression integrated along the adiabatic path.

Second moment of the generator

The second moment of the generator is given by

$$\langle \hat{G}^2 \rangle = \int_0^T \int_0^T \langle \psi_0(0) | \hat{A}_H(t) \hat{A}_H(t') | \psi_0(0) \rangle dt dt'. \quad (\text{C11})$$

Inserting the resolution of the identity

$$\hat{\mathbb{I}} = \sum_n |\psi_n(0)\rangle \langle \psi_n(0)|, \quad (\text{C12})$$

we obtain

$$\langle \hat{G}^2 \rangle = \sum_n \int_0^T dt \int_0^T dt' \langle \psi_0(0) | \hat{A}_H(t) | \psi_n(0) \rangle \langle \psi_n(0) | \hat{A}_H(t') | \psi_0(0) \rangle. \quad (\text{C13})$$

Using the adiabatic approximation for the matrix elements,

$$\langle \psi_0(0) | \hat{A}_H(t) | \psi_n(0) \rangle \approx e^{i[\theta_0(t) - \theta_n(t)]} \langle \psi_0(t) | \partial_\omega \hat{H}(\omega, t) | \psi_n(t) \rangle, \quad (\text{C14})$$

the double time integral factorizes, yielding

$$\langle \hat{G}^2 \rangle \approx \sum_n \left| \int_0^T e^{i[\theta_0(t) - \theta_n(t)]} \langle \psi_0(t) | \partial_\omega \hat{H}(\omega, t) | \psi_n(t) \rangle dt \right|^2. \quad (\text{C15})$$

Here we retain only the leading adiabatic contribution and neglect non-adiabatic corrections, which are suppressed by inverse powers of the instantaneous energy gap.

Variance and quantum Fisher information

The variance of the generator,

$$\Delta^2 \hat{G} = \langle \hat{G}^2 \rangle - \langle \hat{G} \rangle^2, \quad (\text{C16})$$

determines the quantum Fisher information via $\mathcal{I}_\omega = 4 \Delta^2 \hat{G}$. Combining the results above, the diagonal contribution ($n = 0$) cancels identically, yielding

$$\Delta^2 \hat{G} \approx \sum_{n \neq 0} \left| \int_0^T e^{i[\theta_0(t) - \theta_n(t)]} \langle \psi_0(t) | \partial_\omega \hat{H}(\omega, t) | \psi_n(t) \rangle dt \right|^2, \quad (\text{C17})$$

where T is the length of the adiabatic time evolution related to the gap inverse [compare with Eq. (A1)]. The orientation of squeezing in the ground state does not matter as rotating the squeezed vacuum with $\hat{a}^\dagger \hat{a}$ for a harmonic oscillator does not change the expectation value of $\hat{a}^\dagger \hat{a}$ and similar for spin-squeezed states. In critical metrology T is very large due to closing energy gap which increases the quantum Fisher information, while in anti-critical metrology T is very small due to opening of the energy gap which reduces the quantum Fisher information.

No matter how optimal the adiabatic ramp is, the quantum Fisher information for an adiabatic time evolution connecting two neighboring ground states will be

$$\mathcal{I}_\omega = 4 \sum_{n \neq 0} \frac{|\langle \psi_n(\omega) | \partial_\omega \hat{H}(\omega) | \psi_0(\omega) \rangle|^2}{[E_n(\omega) - E_0(\omega)]^2}. \quad (\text{C18})$$

Appendix D: Lipkin-Meshkov-Glick model

In the main text, we have focused on a pedagogical example of the quantum Rabi model, which can be understood from the viewpoint of an elementary harmonic oscillator. Here, we elucidate the principle of anti-critical metrology using a many-body quantum system of interacting identical and indistinguishable spins. Specifically, we consider a symmetric all-to-all interacting Lipkin-Meshkov-Glick model

$$\hat{H} = \omega \hat{S}_z - \frac{g}{N} \hat{S}_x^2, \quad (\text{D1})$$

where $\hat{S}_\alpha = \frac{1}{2} \sum_{i=1}^N \hat{\sigma}_\alpha$ with $\alpha = x, y, z$ are the collective spin operators, ω is the natural spin frequency, g is the interaction strength, and N is the number of spins. Importantly, we restrict our analysis to the symmetric subspace of the Hilbert space, i.e., states with maximal total spin $S = N/2$, which are fully symmetric under particle exchange and capture the collective behavior relevant for critical and anti-critical metrology.

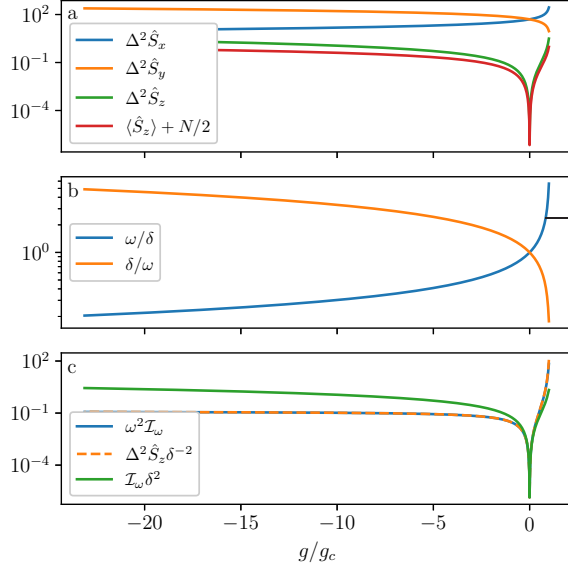


FIG. 3. Lipkin-Meshkov-Glick model. (a) Variances of collective spin components as a function of g/g_c ($g_c \equiv \omega$). The variances of \hat{S}_x (blue line) and \hat{S}_y (orange line) are flipped with respect to each other which shows that quantum correlations can be generated close and away from the critical point. The variance of \hat{S}_z (green line) grows both close and away from the critical point similarly as its expectation value (red line shifted by $N/2$ for the matter of presentation). (b) The associated energy gap (blue line) and its inverse (orange line) are very closely related to variances of \hat{S}_x and \hat{S}_y which points at a close connection between these quantities. Finally, in (c), we show the quantum Fisher information (blue line) as a function of g/g_c which is related to the expectation value of \hat{S}_z weighted by the squared inverse of the energy gap (dashed orange line). Naively it seems that the quantum Fisher information is superior close to the critical point, however, this is caused by the fact that the characteristic time scale artificially elevates the quantum Fisher information. Once the characteristic time is factored out (green line), it turns out that quantum Fisher information can be equally large far away from the critical point and achieved much faster due to decreasing energy gap.

In principle, the Lipkin-Meshkov-Glick model can be considered in the thermodynamic limit, where there exists a mapping to a harmonic oscillator. Here, however, we deliberately perform numerical calculations on $N = 200$ spins to show that a system does not have to map to a harmonic oscillator to benefit from the anti-critical metrology approach. The behavior of the energy gap, the variances of collective spin operators (related to spin squeezing), and the quantum Fisher information both near and away from the critical point are shown in Fig. 3. The variances of the collective spin components in the ground state [panel (a)] closely follow the energy gap between

the ground and first excited states, $\delta = E_1 - E_0$ [panel (b)]. Panel (c) illustrates that the quantum Fisher information (blue line) is essentially the variance of \hat{S}_z weighted by the inverse square of the energy gap (orange dashed line). The naive enhancement of the quantum Fisher information near the critical point therefore arises primarily from the closing of the gap, which lengthens the characteristic time scale of the dynamics. Conversely, away from criticality, the gap increases, reducing the relevant time scale and leading to a smaller, approximately constant quantum Fisher information despite increasing $\Delta^2 \hat{S}_z$. When the quantum Fisher information is normalized by this time scale (green line), it simply recovers the spin variance $\Delta^2 \hat{S}_z$, which can remain large even far from the critical point [green line in Fig. 3a].

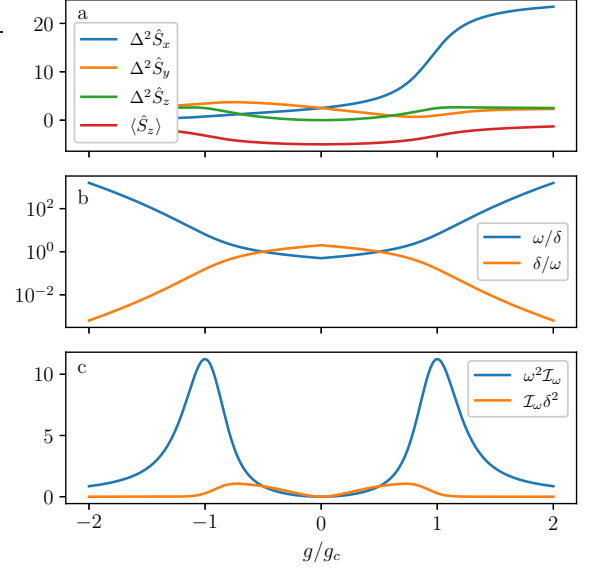


FIG. 4. Transverse field Ising model. (a) Variances of \hat{S}_x (blue line), \hat{S}_y (orange line), and \hat{S}_z (green line) as well as expectation value of \hat{S}_z (red line) as a function of g/g_c . As can be seen, correlations can be equally large close and away from the critical point $g/g_c = 1$. However the energy gap (b) is symmetric with respect to $g/g_c = 0$ point so the gap never increases with increasing coupling. In (c), we see the effect on the quantum Fisher information (blue line) which is symmetric because the correlations depend on $|g/g_c|$, and once divided by the energy gap (orange line) is also symmetric because the gap also depends on $|g/g_c|$ and not on its sign. In this case, anti-critical metrology approach cannot work. In the simulations we have set $N = 10$.

Appendix E: Transverse field Ising model

Now let us turn to another paradigmatic model exhibiting a quantum phase transition, namely, the transverse-field Ising model with nearest-neighbor interactions. The Hamiltonian of the model reads

$$\hat{H} = \omega \sum_{i=1}^N \hat{\sigma}_z^{(i)} - g \sum_{i=1}^N \hat{\sigma}_x^{(i)} \hat{\sigma}_x^{(i+1)}, \quad (\text{E1})$$

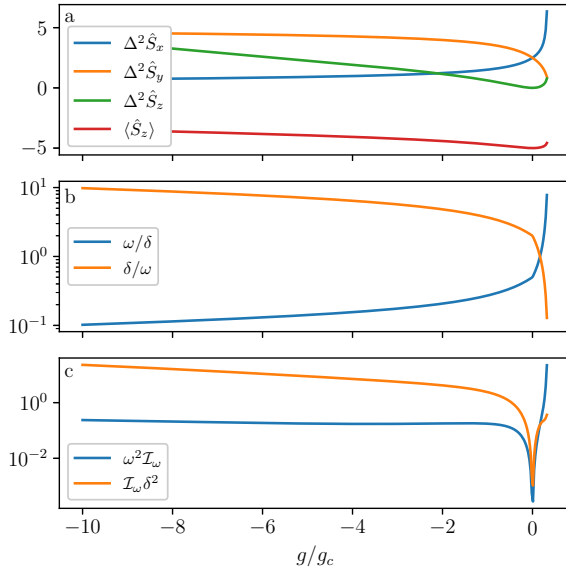


FIG. 5. Transverse field Ising model with transverse interactions. (a) Variances of \hat{S}_x (blue line), \hat{S}_y (orange line), and \hat{S}_z (green line) as well as expectation value of \hat{S}_z (red line) as a function of g/g_c . As can be seen, again correlations can be equally large close and away from the critical point $g/g_c = 1$. However, the energy gap (b) is asymmetric with respect to $g/g_c = 0$ point so the gap can increase with the increasing coupling. In (c), we see the effect on the quantum Fisher information (blue line) which is now asymmetric because the correlations depend on g/g_c in a different way than the gap. In this case, anti-critical metrology approach can work as evidenced by the quantum Fisher information divided by the energy gap (orange line). In the simulations we have set $N = 10$.

where g denotes the strength of the spin–spin interaction, and we have assumed periodic boundary conditions, $\hat{\sigma}_x^{(N+1)} \equiv \hat{\sigma}_x^{(1)}$. The system undergoes a quantum phase transition at the critical point $g = \omega$, separating the paramagnetic and ferromagnetic phases.

For the anti-critical metrology protocol to be effective, many-body interactions must open a finite energy gap that stabilizes the correlated phase away from criticality. However, as illustrated in Fig. 4, this mechanism is not univer-

sal. In the case of the transverse field Ising model, the energy gap inevitably closes regardless of the interaction strength [see Fig. 4b] similar as in the quantum Rabi model from the main text if the spin is in its ground state. Consequently, this model does not allow for an anti-critical regime where strong correlations coexist with a increased excitation gap [see Fig. 4c].

Appendix F: Transverse field Ising model with transverse interactions

The lack of an energy gap opening can be fixed by adding extra nearest-neighbor interactions in the transverse directions. In this case, the Hamiltonian becomes

$$\hat{H} = \omega \sum_{i=1}^N \hat{\sigma}_z^{(i)} - g \sum_{i=1}^N \left(\hat{\sigma}_x^{(i)} \hat{\sigma}_x^{(i+1)} - \hat{\sigma}_z^{(i)} \hat{\sigma}_z^{(i+1)} \right), \quad (\text{F1})$$

which is a special variant of the anisotropic XYZ model, where the interactions along y direction are absent. Adding transverse interactions is not the only way to increase the energy gap, but here we only want to demonstrate that neither all-to-all interactions nor high symmetry of the eigenstates are necessary to harness the anti-critical metrology framework. In particular, unlike in the Lipkin-Meshkov-Glick model, it is not necessary to restrict the dynamics to the maximally symmetric subspace. The results of numerical simulations for $N = 10$ spins are presented in Fig. 5. In panel (a), we show the build-up of correlations as a function of g/g_c . In panel (b), we show the energy gap and its inverse, which exhibit the desired behavior of growing with respect to the non-interacting case $g = 0$. In panel (c), we show the quantum Fisher information, which is maximal close to the critical point (blue line); however, once divided by the characteristic timescale related to the inverse of the energy gap, we see that the quantum Fisher information can be more optimal away from the critical point where the gap increases (orange line). The results are very similar to the results obtained for the Lipkin-Meshkov-Glick model (see Fig. 3) which confirms that neither long-range interactions nor additional constrains on the symmetry of the eigenstates are required for the anti-critical metrology framework to work efficiently.

[1] V. Giovannetti, S. Lloyd, and L. Maccone, Quantum Metrology, *Phys. Rev. Lett.* **96**, 010401 (2006).
 [2] V. Giovannetti, S. Lloyd, and L. Maccone, Advances in quantum metrology, *Nat. Photonics* **5**, 222 (2011).
 [3] L. Pezzè and A. Smerzi, Entanglement, Nonlinear Dynamics, and the Heisenberg Limit, *Phys. Rev. Lett.* **102**, 100401 (2009).
 [4] M. Zwierz, C. A. Pérez-Delgado, and P. Kok, General Optimality of the Heisenberg Limit for Quantum Metrology, *Phys. Rev. Lett.* **105**, 180402 (2010).
 [5] R. Demkowicz-Dobrzański, J. Kołodyński, and M. Gužă, The elusive Heisenberg limit in quantum-enhanced metrology, *Nat. Commun.* **3**, 1063 (2012).
 [6] H. Grote, K. Danzmann, K. L. Dooley, R. Schnabel, J. Slutsky, and H. Vahlbruch, First Long-Term Application of Squeezed States of Light in a Gravitational-Wave Observatory, *Phys. Rev. Lett.* **110**, 181101 (2013).
 [7] C. L. Degen, F. Reinhard, and P. Cappellaro, Quantum sensing, *Rev. Mod. Phys.* **89**, 035002 (2017).
 [8] L. Pezzè, A. Smerzi, M. K. Oberthaler, R. Schmied, and P. Treutlein, Quantum metrology with nonclassical states of atomic ensembles, *Rev. Mod. Phys.* **90**, 035005 (2018).
 [9] S. Pirandola, B. R. Bardhan, T. Gehring, C. Weedbrook, and S. Lloyd, Advances in photonic quantum sensing, *Nat. Phot.* **12**, 724 (2018).

[10] E. Polino, M. Valeri, N. Spagnolo, and F. Sciarrino, Photonic quantum metrology, *AVS Quantum Sci.* **2**, 024703 (2020).

[11] Y. A. Yang, M. Miklos, Y. M. Tso, S. Kraus, J. Hur, and J. Ye, Clock Precision beyond the Standard Quantum Limit at 10^{-18} level, *Phys. Rev. Lett.* **135**, 193202 (2025).

[12] B. M. Escher, R. L. de Matos Filho, and L. Davidovich, General framework for estimating the ultimate precision limit in noisy quantum-enhanced metrology, *Nat. Phys.* **7**, 406 (2011).

[13] R. Chaves, J. B. Brask, M. Markiewicz, J. Kołodyński, and A. Acín, Noisy Metrology beyond the Standard Quantum Limit, *Phys. Rev. Lett.* **111**, 120401 (2013).

[14] P. Zanardi, M. G. A. Paris, and L. Campos Venuti, Quantum criticality as a resource for quantum estimation, *Phys. Rev. A* **78**, 042105 (2008).

[15] P. Zanardi, P. Giorda, and M. Cozzini, Information-Theoretic Differential Geometry of Quantum Phase Transitions, *Phys. Rev. Lett.* **99**, 100603 (2007).

[16] L. Campos Venuti and P. Zanardi, Quantum Critical Scaling of the Geometric Tensors, *Phys. Rev. Lett.* **99**, 095701 (2007).

[17] G. Mihairescu, U. Alushi, R. D. Candia, S. Felicetti, and K. Gietka, Critical Quantum Sensing: a tutorial on parameter estimation near quantum phase transitions (2025), [arXiv:2510.02035](https://arxiv.org/abs/2510.02035).

[18] L. Ostermann and K. Gietka, Temperature-enhanced critical quantum metrology, *Phys. Rev. A* **109**, L050601 (2024).

[19] U. Alushi, W. Górecki, S. Felicetti, and R. Di Candia, Optimality and Noise Resilience of Critical Quantum Sensing, *Phys. Rev. Lett.* **133**, 040801 (2024).

[20] G. Mihairescu, S. Campbell, and K. Gietka, Uncertain quantum critical metrology: From single- to multiparameter sensing, *Phys. Rev. A* **111**, 052621 (2025).

[21] C. Hotter, A. Miranowicz, and K. Gietka, Quantum Metrology in the Ultrastrong Coupling Regime of Light-Matter Interactions: Leveraging Virtual Excitations without Extracting Them, *Phys. Rev. Lett.* **135**, 100802 (2025).

[22] M. M. Rams, P. Sierant, O. Dutta, P. Horodecki, and J. Zakrzewski, At the Limits of Criticality-Based Quantum Metrology: Apparent Super-Heisenberg Scaling Revisited, *Phys. Rev. X* **8**, 021022 (2018).

[23] V. Montenegro, C. Mukhopadhyay, R. Yousefjani, S. Sarkar, U. Mishra, M. G. Paris, and A. Bayat, Review: Quantum metrology and sensing with many-body systems, *Phys. Rep.* **1134**, 1 (2025), review: Quantum metrology and sensing with many-body systems.

[24] W. Górecki, F. Albarelli, S. Felicetti, R. Di Candia, and L. Maccone, Interplay Between Time and Energy in Bosonic Noisy Quantum Metrology, *PRX Quantum* **6**, 020351 (2025).

[25] M.-J. Hwang, R. Puebla, and M. B. Plenio, Quantum Phase Transition and Universal Dynamics in the Rabi Model, *Phys. Rev. Lett.* **115**, 180404 (2015).

[26] K. Gietka, F. Metz, T. Keller, and J. Li, Adiabatic critical quantum metrology cannot reach the Heisenberg limit even when shortcuts to adiabaticity are applied, *Quantum* **5**, 489 (2021).

[27] Y. Chu, S. Zhang, B. Yu, and J. Cai, Dynamic framework for criticality-enhanced quantum sensing, *Phys. Rev. Lett.* **126**, 010502 (2021).

[28] T. Ilias, D. Yang, S. F. Huelga, and M. B. Plenio, Criticality-Enhanced Quantum Sensing via Continuous Measurement, *PRX Quantum* **3**, 010354 (2022).

[29] L. Garbe, M. Bina, A. Keller, M. G. A. Paris, and S. Felicetti, Critical Quantum Metrology with a Finite-Component Quantum Phase Transition, *Phys. Rev. Lett.* **124**, 120504 (2020).

[30] Q.-Y. Chen, F. Qiao, and Z.-J. Ying, Globalized critical quantum metrology in dynamics of quantum rabi model by auxiliary nonlinear term (2025), [arXiv:2511.14946](https://arxiv.org/abs/2511.14946).

[31] Q. Xie, H. Zhong, M. T. Batchelor, and C. Lee, The quantum Rabi model: solution and dynamics, *J. Phys. A: Math. Theor.* **50**, 113001 (2017).

[32] M. L. Cai, Z. D. Liu, W. D. Zhao, Y. K. Wu, Q. X. Mei, Y. Jiang, L. He, X. Zhang, Z. C. Zhou, and L. M. Duan, Observation of a quantum phase transition in the quantum Rabi model with a single trapped ion, *Nat. Commun.* **12**, 1126 (2021).

[33] J. S. Pedernales, I. Lizuain, S. Felicetti, G. Romero, L. Lamata, and E. Solano, Quantum Rabi Model with Trapped Ions, *Sci. Rep.* **5**, 15472 (2015).

[34] D. Lv, S. An, Z. Liu, J.-N. Zhang, J. S. Pedernales, L. Lamata, E. Solano, and K. Kim, Quantum simulation of the quantum rabi model in a trapped ion, *Phys. Rev. X* **8**, 021027 (2018).

[35] J. Braumüller, M. Marthaler, A. Schneider, A. Stehli, H. Rotzinger, M. Weides, and A. V. Ustinov, Analog quantum simulation of the rabi model in the ultra-strong coupling regime, *Nat. Commun.* **8**, 779 (2017).

[36] K. Gietka, Harnessing center-of-mass excitations in quantum metrology, *Phys. Rev. Res.* **4**, 043074 (2022).

[37] K. Gietka and H. Ritsch, Squeezing and Overcoming the Heisenberg Scaling with Spin-Orbit Coupled Quantum Gases, *Phys. Rev. Lett.* **130**, 090802 (2023).

[38] S. L. Braunstein and C. M. Caves, Statistical distance and the geometry of quantum states, *Phys. Rev. Lett.* **72**, 3439 (1994).

[39] M. G. A. Paris, Quantum estimation for quantum technology, *Int. J. Quantum Inf.* **07**, 125 (2009).

[40] S. Mirkhalaf, H. Ritsch, and K. Gietka, Frequency shifts as a reflection of ground state squeezing and entanglement in two coupled harmonic oscillators (2025), [arXiv:2511.03687](https://arxiv.org/abs/2511.03687).

[41] W. H. Zurek, U. Dorner, and P. Zoller, Dynamics of a Quantum Phase Transition, *Phys. Rev. Lett.* **95**, 105701 (2005).

[42] J. Dziarmaga, Dynamics of a quantum phase transition and relaxation to a steady state, *Adv. Phys.* **59**, 1063 (2010).

[43] A. Polkovnikov, K. Sengupta, A. Silva, and M. Vengalattore, Colloquium: Nonequilibrium dynamics of closed interacting quantum systems, *Rev. Mod. Phys.* **83**, 863 (2011).

[44] K. Gietka, Squeezing by critical speeding up: Applications in quantum metrology, *Phys. Rev. A* **105**, 042620 (2022).

[45] J.-Y. Gyhm, H. Kwon, and M.-J. Hwang, Fundamental Scaling Limit in Critical Quantum Metrology (2025), [arXiv:2506.19003](https://arxiv.org/abs/2506.19003).

[46] P. Forn-Díaz, L. Lamata, E. Rico, J. Kono, and E. Solano, Ultrastrong coupling regimes of light-matter interaction, *Rev. Mod. Phys.* **91**, 025005 (2019).

[47] A. Frisk Kockum, A. Miranowicz, S. De Liberato, S. Savasta, and F. Nori, Ultrastrong coupling between light and matter, *Nat. Rev. Phys.* **1**, 19 (2019).

[48] F. Beaudoin, J. M. Gambetta, and A. Blais, Dissipation and ultrastrong coupling in circuit QED, *Phys. Rev. A* **84**, 043832 (2011).

[49] M. Stefanini, A. A. Ziolkowska, D. Budker, U. Poschinger, F. Schmidt-Kaler, A. Browaeys, A. Imamoglu, D. Chang, and J. Marino, Is Lindblad for me? (2025), [arXiv:2506.22436](https://arxiv.org/abs/2506.22436).

[50] P. Szałkowski, Introduction to the theory of open quantum systems, *SciPost Phys. Lect. Notes* **68** (2023).

[51] C. W. Gardiner and P. Zoller, *Quantum Noise: A Handbook of Markovian and Non-Markovian Quantum Stochastic Methods with Applications to Quantum Optics*, 3rd ed., Springer Series in Synergetics (Springer, Berlin, Heidelberg, 2004) third edition (Aug 27, 2004).

[52] L. Garbe, O. Abah, S. Felicetti, and R. Puebla, Critical quantum metrology with fully-connected models: from Heisenberg to Kibble-Zurek scaling, *Quantum Sci. Technol.* **7**, 035010 (2022).

[53] G. Mihailescu and K. Gietka, Dynamic framework for anti-criticality-enhanced quantum sensing (2026), to be published.